Material characterization of the MSWI bottom ash as a function of particle size. Effects of glass recycling over time

R. del Valle-Zermeño, J. Gómez-Manrique, J. Giro-Paloma, J. Formosa, J.M. Chimenos *

Departament de Ciència dels Materials i Química Física, Facultat de Química, Universitat de Barcelona, Martí i Franquès, 1, E-08028 Barcelona, Spain

HIGHLIGHTS

- The content of glass in particles N 16 mm has decreased in weathered bottom ash (WBA).
- Entire glass bottles have been easily recycled and extensively substituted by plastic.
- There's still a significant amount of glass that's left unrecycled: 60.8%.
- Ceramics are currently the major phase in WBA coarse fractions.
- The finest fractions are the major contributors to the heavy metals content.

GRAPHICAL ABSTRACT

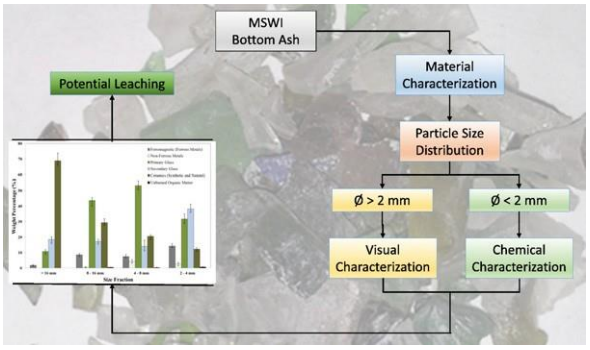

article info

Article history:
Received 27 July 2016
Received in revised form 20 December 2016
Accepted 7 January 2017
Available online 12 January 2017

Editor: Simon Pollard

Keywords:
Bottom ash
Material characterization
Particle size distribution
Glass recovery
Secondary building material

abstract

Differences during the last 15 years in materials' composition in Municipal Solid Waste Incineration (MSWI) regarding bottom ash (BA) were assessed as a function of particle size (N 16, 8–16, 4–8, 2–4, 1–2 and 0–1 mm). After sieving, fractions N 2 mm were carefully washed in order to separate fine particles adhering to bigger particles. The characterization took into account five types of materials: glass (primary and secondary), ceramics (natural and synthetic), non-ferrous metals, ferrous metals and unburned organic matter. The evaluation was performed through a visual (N 2 mm) and chemical (0–2 mm) classification. Results showed that total weight of glass in the particles over 16 mm has decreased with respect to 1999. Moreover, the content of glass (primary and secondary) in BA was estimated to be 60.8 wt%, with 26.4 wt% corresponding to primary glass in N 2 mm size fractions. Unlike 1999, in which glass was the predominant material, ceramics are currently the major phase in bottom ash (BA) coarse fractions. As for the metals, respect to 1999, results showed a slight increase in all size fractions. The greatest content (N 22 wt%) of ferromagnetic was observed for the 2–4 mm size fraction while the non-ferrous type was almost non-existent in particles over 16 mm, remaining below 10 wt% for the rest fractions. In the finest fractions (b 2 mm), about 60 to 95% of non-ferrous metals corresponded to metallic aluminium. The results from the chemical characterization also indicated that the finest fractions contributed significantly to the total heavy metals content, especially for Pb, Zn, Cu, Mn and Ti.

1. Introduction

In the last two decades, the world's most industrialised countries have made great efforts to increase recycling rates of Municipal Solid Waste (MSW) and reduce waste disposal. Their national laws define a

* Corresponding author.
E-mail addresses: delvallezermeno@gmail.com (R. del Valle-Zermeño), judit_gomez_mque@ub.edu (J. Gómez-Manrique), jessicagiro@ub.edu (J. Giro-Paloma), joanformosa@ub.edu (J. Formosa), chimenos@ub.edu (J.M. Chimenos).

hierarchy that sets down the priorities in waste management policies: prevention, reuse, recycling (including composting), energy valorization and finally disposal. For instance, during the last years in Catalonia (Northeast of Spain) recycling rate has improved significantly from 17.7% in 2000 to 37.9% in 2013 (ARC, 2016).

MSW can be classified in recyclable and non-recyclable or refuse materials. The former allows extending the service life of materials while reducing the air emissions and energy inputs derived from processing naturally occurring raw materials (Roy, 1996). As for the latter, incineration has become the most preferred alternative with respect landfilling, as it allows reducing the waste volume and weight (Bontempi et al., 2010; Puma et al., 2013). Bottom ash (BA) is the most significant by-product from MSW incineration (MSWI) as it accounts for 85–95% of the solid product resulting from combustion and is considered a slag and granular material (Chandler et al., 1997; Izquierdo et al., 2002). The EU policy of resource-efficiency has triggered the reuse of stabilized BA as secondary building material for road construction and in concrete or cement production (Chimenos et al., 1999; Grosso et al., 2011; Monteiro et al., 2006). Environmental and mechanical properties are directly dependent on BA composition, which is a mixture of calcium-rich compounds and others silicates enriched in iron and sodium (Freyssinet et al., 2002).

The effectiveness of recycling should have a direct effect on refuse composition and therefore on BA. Among the different recyclable materials, glass stands out because its recycling is supported by the solid waste management industry (Tchobanoglous et al., 1994). This relies in the fact that glass packaging is 100% recyclable and can be recycled repeatedly (Roy, 1996). Moreover, burning glass in waste-to-energy plants does not provide any heat energy for making steam or electricity (Miller, 1995).

Curbside collection systems are the most efficient way to collect all types of glass containers (Miller, 1995). In Catalonia, glass recycling started in 1982 and they have experienced a great increase during the last decade, achieving 20.9 kg of glass recycled per person by 2013. This ratio is greater than the national average (14.5 kg·person^{-1}) and lower than other EU27 countries, like (values per capita) Belgium (35 kg), France (31 kg), Germany (29 kg), the UK (28 kg) and Austria and Ireland (27 kg) (ARC, 2016; Eurostat, 2016).

The Catalan Waste Agency (ARC) has promoted curbside collection of five different fractions in five different containers: plastic packaging, paper and cardboard, packaging glass, organic fraction, and refuse. MSW refuse fraction is disposed in landfills (37.0%), sorted in mechanical biological treatment plants (MBT; 52.4%) to further remove recyclable elements and to stabilize the biodegradable organic fraction, or taken to waste-to-energy incineration plants (MSWI; 10.6%). Considering all waste streams in Catalonia for 2013, 17.7% of MSW was managed in waste-to-energy plants, 41.3% was landfilled and the remainder (41.0%) was recovered, reused or recycled.

At present, the average content of glass in the refuse fraction in Catalonia is 8.3% (PRECAT20, 2012). Following glass recyclability, aluminium recovery has also been long practiced because it is easy to reuse and allows saving up to 95% of energy (Hu et al., 2011; Zhou et al., 2006). Its recovery also improves BA quality for road constructions by avoiding swelling and expansion (Biganzoli et al., 2014; Biganzoli et al., 2013). The scraps are separated by Eddy current separators (EC) on particle size fractions over 5 to 8 mm (Biganzoli et al., 2014). Thus, significant amounts of metallic Al remained uncollected (Berkhout, 2011). Factually, N 90% of the total aluminium (metal and Al-compounds) is found in the fraction below 1 mm and it is mainly regarded to come from light packaging and Al foils (Biganzoli et al., 2013). The metallic Al recovering in Catalonia has the highest rate of Spain, 1117 tons per year by 2008, which accounted to be 24.2% with respect the rest of the country. However, its evolution during the last years has experienced a decrease of 42.7% from 2002 to 2012, with a current mass of 688 tons of packaging aluminium (ARPAL, 2012).

In 1999, a chemical characterization of BA from two MSWI facilities located in Catalonia was carried out by Chimenos (Chimenos et al., 1999). The particles with a diameter N 1 mm were characterized by identifying the main constituents (glass, magnetic metals, diamagnetic metals, synthetic ceramics, unburned organic matter and minerals). According to this study, glass was the main material among all size fractions, and it was regarded to come from domestic items such as beverage bottles and food packaging containers (Chimenos et al., 1999). A decade later and outside EU countries, other authors have also reported that glass is still the main BA constituent, approximately 50 wt% (Wei et al., 2011). Fifteen years have passed since the authors presented this characterization study, and the current BA composition is expected to be quite different as a result of the recycling programs, among others, followed during the last years.

The aim of this study was to perform a new BA materialographic characterization as a function of particle size, in order to identify the differences in composition as a result of recycling tendencies. However, although all the materials previously studied in 1999 were characterized (Chimenos et al., 1999), only data from public administration on glass recycling over time are available. Thus, recycling data of the last years was used to relate the effect of the voluntary recycling programs of glass and its content in BA. Besides, the efficiency of conventional metals recovering methods through separation devices located in the conditioning plants of the BA was assessed.

2. Materials and methods

2.1. MSWI BA sampling

The samples of BA were collected from an energy-to-waste facility located in Tarragona (Spain). Two types of residues are produced: fresh quenched bottom ash (FBA) and air pollution control fly ashes (APC). Although the incineration plant manages each year, approximately, the same amount (140,000 tons) of MSW (refuse fraction), the FBA generated during the last 15 years has significantly decreased (around 3 wt%), as it can be seen in Fig. 1. The same figure shows that APC has increased around 0.75 wt% in the same period. These facts may be directly related to curbside collection programs for recoverable end-of-life materials, such as glass, metals or packages. Most of these end-of-life materials are non-combustibles, and these voluntary collection programs prevented them to end in FBA after incineration. In contrast, a higher percentage of combustible material in MSW (refuse fraction) generates more acid gases (CO_2, SO_2, HCl), which also produces a greater amount of APC ashes.

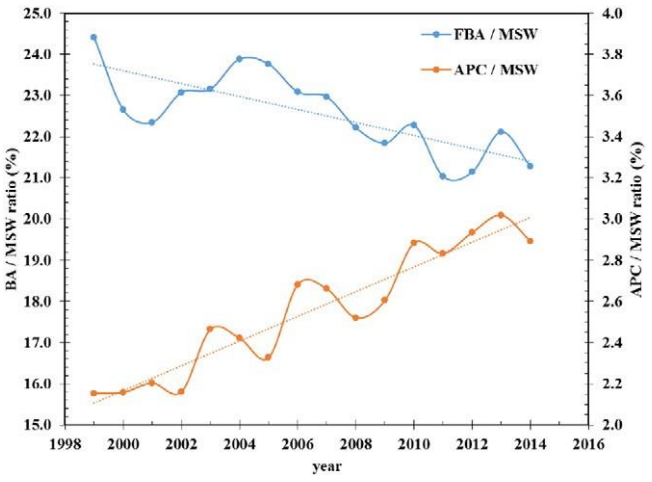

Fig. 1. Percentage of fresh bottom ash (FBA) and air pollution control fly ash (APC) generated in the incineration process of Municipal Solid Waste (MSW) over the last 15 years. Source: SIRUSA.

This facility managed 140,322 tons of MSW (refuse fraction) during 2013, producing 2467 tons of residual metallic material larger than 250 mm and 31,037 tons of FBA. The latter is further processed in a conditioning plant for the recovery of some valuable materials (ferrous and non-ferrous metals) and for obtaining a homogenized granular material (GM). After stabilization (natural weathering), GM is fully reused as secondary building material. It was during the homogenization and conditioning process where sampling, by triplicate, took place over one week. Two sampling points were placed (Fig. 2): (i) on the drag conveyor after the first screening (b 30 mm) entering the hopper from the trommel. Samples taken at this point were labelled as "A" (see Fig. 2). The oversize fraction (N 30 mm) represents b 2 wt% of the total collected FBA and hence it was not considered in this study. (ii) at the end of the conditioning process after metal separation devices (two magnetic and one Eddy current separators), sampling point "D" (see Fig. 2). The samples taken at points A and D belong to the same batch. By this manner, 25 kg of each sample (A and D) were taken every hour (1, 2, and 3) during three hours each day, with a total amount of six samples per day (~75 kg each) for each A and D samples.

2.2. BA materialographic characterization

Each sample was homogenized and quartered repeatedly to reduce the weight prior taking representative sub-samples of about 5 kg for the materialographic classification. The particle size distribution of each sub-sample was determined by the same procedure as in previous research work (Chimenos et al., 1999). This consisted in sieving with openings standards of 0.063, 1, 2, 4, 8 and 16 mm (EN 933-2). After sieving, each fraction (N16, 8–16, 4–8, 2–4, 1–2 and 0–1 mm) was washed with water (L/S ≈ 5, continuously stirred during 30 min) in order to separate the fines adhered to coarse particles. The samples with a particle size between 2 and 4 mm were further carefully washed with 0.1 M hydrochloric acid for better classification as well as to dissolve the fine alkaline particles adhering to the surface (Chimenos et al., 1999).

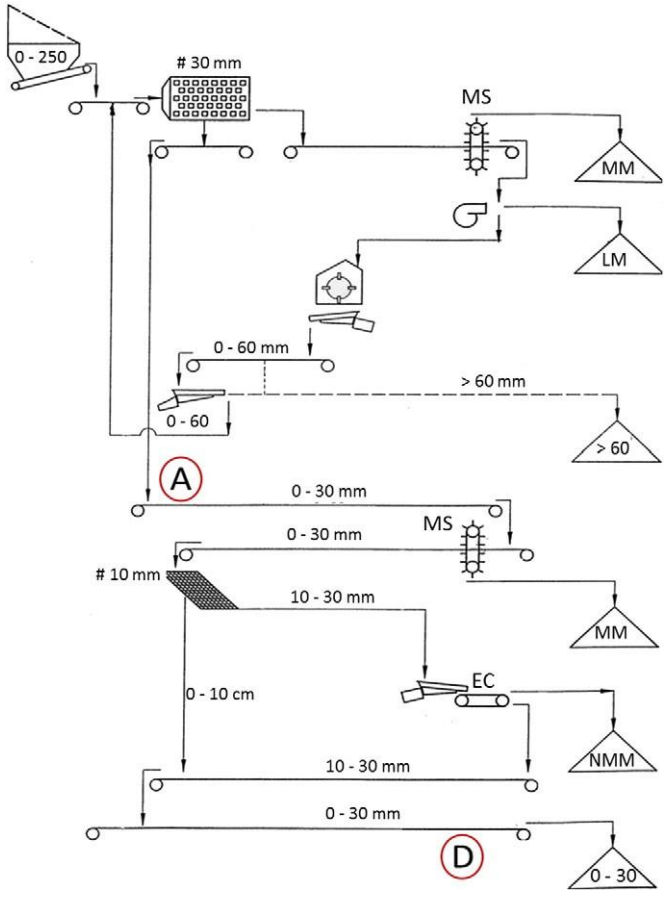

Fig. 2. Scheme of the conditioning plant where sampling took place. Sampling points A (discharged from the trommel) and D (outlet) are marked for better understanding. MS: magnetic separator; MM: magnetic metals; LM: light materials; EC: Eddy current; NMM: Non-magnetic Metals.

Then, each size fraction was dried at 105 °C for 24 h and weighed. The samples with a particle size above 4 mm were classified visually while those into 2–4 mm fraction were classified using a magnifying glass. The classification took into account five types of materials: glass (primary and secondary), ceramics (natural and synthetic), non-ferromagnetics (non-ferrous metals), ferromagnetics (ferrous metals), and unburned organic matter (OM). The major source of glass in MSWI BA comes from packaging glass, called primary glass, which mainly has the same composition of soda-lime glass. This may remain unchanged during the combustion process. However, BA also contains secondary glass, which is newly-formed during the combustion process at high temperatures (Zevenbergen et al., 1996). The latter is more fragile, contains large amounts of porosity (gas bubbles), vesicles and cracks, as well as inclusions of other materials. Its source may be the primary glass, but also other silicates or silica contained in MSW.

Ferromagnetics were collected by placing a magnet (Nd; 0.485 T) over the spread sample at 10 mm height distance. The organic matter content in the 0–2 mm fractions was determined following the UNE 103204:93, where potassium permanganate is used as an oxidizing reagent (AENOR, 1993). The contents of metallic aluminium and glass in the finest fractions (b 2 mm) was estimated through chemical and crystallographic methods respectively, as it will be addressed in the next section.

2.3. Chemical determination of metallic aluminium in the finest fractions

The visual quantification of non-ferrous metals in b 2 mm BA fractions was not feasible. In these particle size fractions, the main source of non-ferrous metals is aluminium foil. There are other non-ferromagnetic metals such as copper and its alloys (bronze and brass) with Al/Cu ≈ 17:1 (Chimenos et al., 2003). It can be assumed that the large majority of non-ferrous metals in the size fractions lower than 2 mm is aluminium. In this hypothesis, the quantification of metallic aluminium was carried out using the soda attack method. This method is based on measuring the H_2 released by the reaction of metallic Al with NaOH (Eq. (1)), as reported elsewhere (Berkhout, 2011; Biganzoli et al., 2013; Hu et al., 2011):

$$2Al + 2OH^- + 2H_2O \rightarrow 2AlO_2^- + 3H_2 \quad (1)$$

Approximately 5 ± 0.5 g of D samples with different fine size fractions (0–1 and 1–2 mm) was weighted separately (in triplicate) and put in contact with 200 ml of 1.0 M NaOH in a flask under constant agitation. The open end of the flask was connected to a graduated cylinder that was placed upside down inside a beaker full of water. Prior to each experimental trial, a vacuum was created inside the graduated cylinder in contact with water and the initial column of water was measured. The volume of H_2 produced displaced the column of water. The total consumption of metallic Al was considered the end of the reaction, when the column of water remained still for more than two hours. Then, the percentage of metallic Al was calculated according to Eq. (2):

$$Al(\%) = \frac{1.5 \times P \times \Delta V}{R \times T \times M_{Al} \times m} \times 100 \quad (2)$$

where P is the atmospheric pressure (atm), ΔV is the difference between the initial and final volume of water column, R is the gas constant (0.082 l·atm·mol^{-1}·K^{-1}), T is temperature (K), M_{Al} is the molar mass of metallic Al (26.9 g·mol^{-1}) and m is the mass of the BA sample (g) of each experimental trial.

2.4. Crystallographic determination of glass in the finest fractions

The glass content in the 0–2 mm size fraction was quantitatively determined using X-ray diffractometry (XRD), based on the analysis developed by Rietveld (1969). In addition, the Rietveld analysis also allows estimating the proportions of any amorphous or non-crystalline material (Ward and French, 2006). The analysis was carried out in a Bragg–Brentano Siemens D-500 powder diffractometer device with CuKα radiation. The identification of all minerals was made with X'Pert HighScore software and PDF-2 2006 database (ICDD, 2006). Subsequently the sample was mixed with Al_2O_3 NIST SRM-676a (25 wt%) for both qualitative and quantitative analysis. The Rietveld method was performed on the diffraction pattern of the sample with Al_2O_3 (25 wt%) using FullProf program. With this purpose, a dry sub-sample of about 50 g was ground using a ball mill for obtaining the optimum particle size (1 μm) for X-ray diffraction analysis.

BA can be regarded as crystalline and non-crystalline components. It can be assumed that all the amorphous phases are due to the presence of glass (primary or newly-formed). The quantification of amorphous phases may be used for quantifying the glass content. The assumed error in this statement is likely lower than the uncertainty introduced by the heterogeneity of the samples or the analytical methodology.

2.5. Distribution of heavy metals in the different size fractions

Although the use of total concentration as the criterion for assessing the potential effects of heavy metals and metalloid is clearly incorrect, because it assumes that all forms and mineralogical phases have the same availability, this parameter is appropriate to assess the potential leaching of these elements. Accordingly, to determine the potential leaching of heavy metals and metalloids, each size fraction was crushed and milled (when necessary) to a size below 2 mm. Between 5 and 10 g of each size fraction were digested per duplicate using hot concentrated nitric acid. The concentration of Pb, Zn, Cu, Ti, Cr, Mn, Co, Ni, As, Mo, Cd, Sn, Sb, Ba, W and Bi was determined by Inductive Coupled Argon Plasma Atomic Emission Spectrometer (ICP-AES).

The organic matter of the finest fractions (0–1 and 1–2 mm) was determined according to the UNE 103204:93, where potassium permanganate is used as oxidizing reagent of organic matter (AENOR, 1993).

3. Results and discussion

3.1. Particle size distribution (PSD)

Fig. 3 shows the grading curve of samples at the entrance (A) and outlet (D) of the recovery process. A comparison with an optimum grading distribution depicted by the Fuller curve is also presented. Well-graded aggregates tend to be less prone to changes in volume (densification) due to re-arranging of the particles than uniform aggregates. Accordingly, to achieve a well-graded aggregate, this comparison evaluates the BA suitability as alternative material for road constructions (Ginés et al., 2009).

Up to about 50 wt% of the BA is made up of particles ≥ 4 mm. The particle size distribution (PSD) is very similar to the data obtained from the same waste-to-energy plant in 1999 (Chimenos et al., 1999). Thus, despite recycling programs, PSD has not varied significantly. Consequently, PSD is rather related to the attrition between the particles and the moving grate (rotating rolls) inside the combustion chamber.

Moreover, size fraction decreases downstream, as the percent passing increases as the samples travelled through the drag conveyor. For better understanding, point 1 in Fig. 3 (sampling point D) indicates that 92 wt% of the sample passed through the 16 mm mesh, while that of point 2 (sampling point A) was close to 87 wt%, which means that 13 wt% of the sample had a size over 16 mm. This fact was especially relevant for all size fractions over 8 mm, since ferrous (ferromagnetic metals) and non-ferrous metals were recovered by electromagnets and EC from the ≥ 10 mm material stream (see flowchart in Fig. 2). The 1–2 and 2–4 mm size fractions were very similar between both sampling points, since they were not affected by the multiple screenings and separation devices placed downstream. Although the two samples of BA showed a good match to the Fuller curve, there is an excess of the coarse particles and lack of fines below 0.15 mm.

3.2. Materialographic classification

3.2.1. Samples at the entrance of the recovery process

Fig. 4 shows the average results of the visual quantification (2–30 mm) of the samples at the entrance of the conditioning plant (samples A). The results were very similar among replicates, which allows considering a good reproducibility. It is quite noticeable the highest

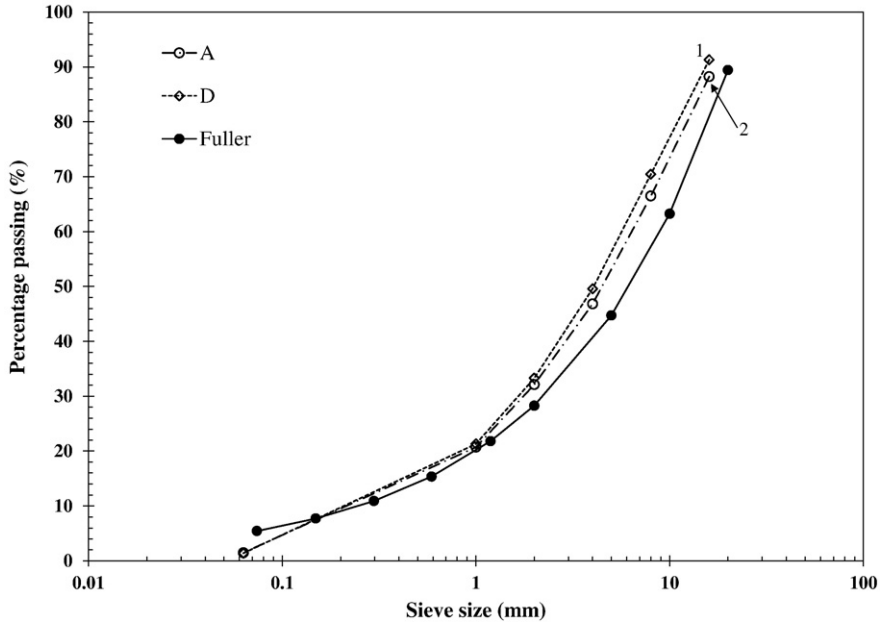

Fig. 3. Curves of particle size distribution (percent passing vs. sieve size) for the samples at the entrance of the recovery process (A) and at the outlet (D). The comparison with the Fuller curve is also presented.

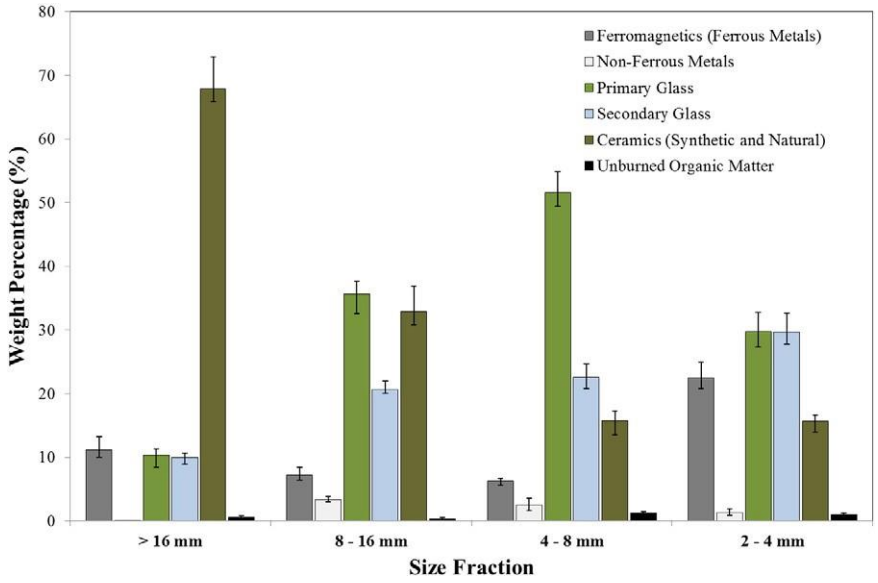

Fig. 4. Distribution of materials as a function of particle size (N 2 mm) in the MSWI bottom ash at the entrance of recovery process at the conditioning plant (sample A).

percentage of ceramics in the coarse fraction (N 16 mm) which was comprised between 65 and 72 wt% of the total content and gradually decreased along the size fraction. The main components were fragments of cement, concrete, brickbat or gypsum, from small refurbishment works of domestic properties, and pottery, and porcelain (Fig. 5). The values are substantially higher than those previously reported by Chimenos et al. (1999), revealing the greater role that ceramics play in the current BA composition as they are not implemented in any specific take-back or curbside voluntary recycling program.

The greatest content of ferrous metals (ferromagnetic) was observed for the 2–4 mm (exceeded the 22 wt%) and coarse fractions (N 16 mm; 11 wt%). It should be emphasized that the nature of coarse ferrous metals and those presented in the fine fractions was significantly different. The coarse fractions were mainly formed by pieces of steel and iron that superficially oxidized in the combustion furnace. On the other hand, small particles, e.g. magnetized sand or iron filings were predominantly present in the 2–4 mm fraction.

Fig. 5. Ceramic materials contained in the coarse fraction (N 16 mm). This picture was taken from a previously washed fraction.

As for the non-ferromagnetic fraction, metallic aluminium is the most relevant fraction (70 wt% on average) of non-ferrous metals, while metals such as copper, brass, etc. are present in lower amounts (Biganzoli and Grosso, 2013). Non-ferrous metals were almost non-existent in the N 16 mm fraction. Its content slightly increased with decreasing size fraction, being below 10 wt%.

The quantity of unburned matter ranged from 0.6–1.25 wt%, presenting the highest values for the 8–4 mm fractions. These values were of the same order as those presented 15 years ago. Basically, the unburned matter consisted of plastic trash bags, synthetic fibres, wood fragments and carbonaceous semi-burned particles (Chimenos et al., 1999). It has to be highlighted that the Spanish Technical Specifications for Road Construction PG3 set a limit of 2% of organic matter in BA for road constructions (Ministerio de Fomento, 2010).

The vast majority of glass particles remain unchanged during incineration, while others acquire a certain viscosity and modify their original morphology by partial meltdown. Accordingly, in order to assess glass content, unchanged particles of glass bottles and coloured packaging glass were considered as primary while melted and newly-formed glasses were considered the secondary kind (Fig. 6). As it is shown in Fig. 4, the content of glass (primary and secondary) is over 50 wt% in all particle size fractions, except for those larger than 16 mm. In reference to the results in 1999, the substantial decrease in the total weight for the coarse particles can partly be explained by the fact that entire glass bottles (beer, wine and other food and beverage packaging) are easily stored in domestic houses and further collected at curbside. Broken glass bottles are not recycled and are disposed as refuse instead. This explains the similarity to the 1999 study of primary glass values in the 8–16 and 4–8 mm fractions. The content of primary and secondary glass is similar for N 16 mm and 2–4 mm fractions. However, the percentage of secondary glass phases cannot be entirely related to glass packaging and hence recycling, as many of the silicates forming amorphous secondary phases might come from other sources.

Since the percentage of the finest fraction (0–2 mm) is not affected by metal recovery processes (see Figs. 2 and 3), the further section addresses the materialographic study of the samples at the outlet of the recovery process.

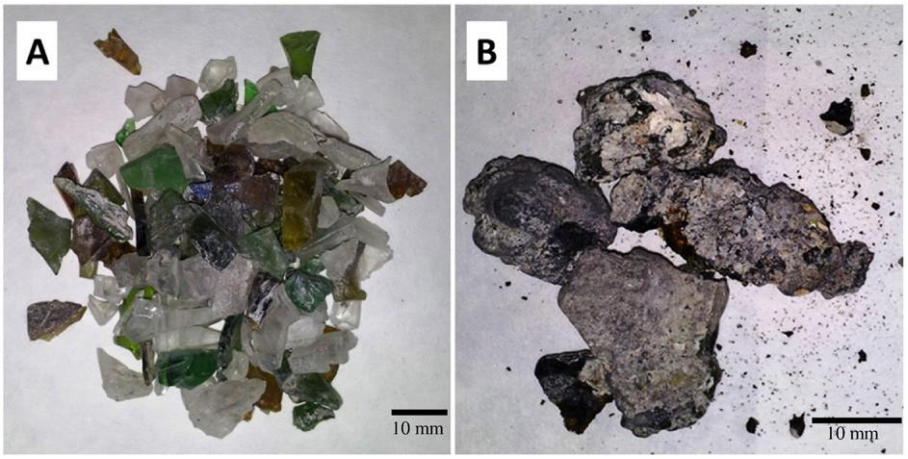

Fig. 6. Primary (A) and secondary glass (B) contained in 4–8 mm size fraction. This picture was taken from a previously washed fraction.

3.2.2. Samples at the outlet of the recovery process

Fig. 7 presents the average of visual quantification (2–30 mm) of the materials comprising the samples at the outlet (sample D). The greatest differences between Figs. 4 and 7 are related to the proportional amounts of each material in coarser fractions (sizes over 8 mm), where the recovery devices are more effective (see Fig. 2). There was a substantial decrease (~10 wt%) in the ferromagnetic content for the N 16 mm fraction and a complete recovery of the total content of non-ferrous metals (mainly metallic aluminium) and discards of unburned organic matter. Consequently, the relative content of ceramics and the two types of glass increased. Hence, the MS and EC placed between both sampling points proved to be very effective for particles with sizes over 16 mm. A decrease in the separation efficiency for the 8–16 mm fraction was detected, as 8.6 and 0.5 wt% remained for ferromagnetic and non-ferrous metals, respectively. Primary glass remained as the major material in the 8–16 mm fraction, although its relative content slightly increased. The proportion of materials in the 4–8 mm fraction was very similar to the corresponding to the samples at the entrance. Hence, the recovery method (electromagnet) is regarded to be ineffective for size particles below 8 mm. The slight unexpected decrease in ferromagnetic metals in the 2–4 mm fraction can be related to BA heterogeneity as well as the slight increase in non-ferrous metals. The main components in this fraction were again glass and ceramics, despite the secondary glass content was slightly higher (~ 38.3 wt%), showing the melting process that partially acts on the glass finest particles.

The materialographic characterization of sample D also includes thermal and chemical characterization as well as XRD analysis in 0–2 mm size fraction. This allowed the quantification of unburned OM, the content of non-ferrous metals (metallic Al), and glass (primary and secondary), respectively.

3.2.2.1. Content of metallic aluminium in the finest fractions. Prior to the chemical determination of metallic aluminium in the 0–2 mm size fraction by means of the soda attack method (Eq. (2)), the same visual quantification procedure was carried out in the 2–4 mm fraction of sample D (see Fig. 7). An average content of 1.94 ± 0.22 wt% was determined for the 2–4 mm fraction, which was in the same order of magnitude, but slightly lower than the percentage of non-ferrous metals (2.76 ± 0.92 wt%). Accordingly, about 60 to 90% of non-ferrous

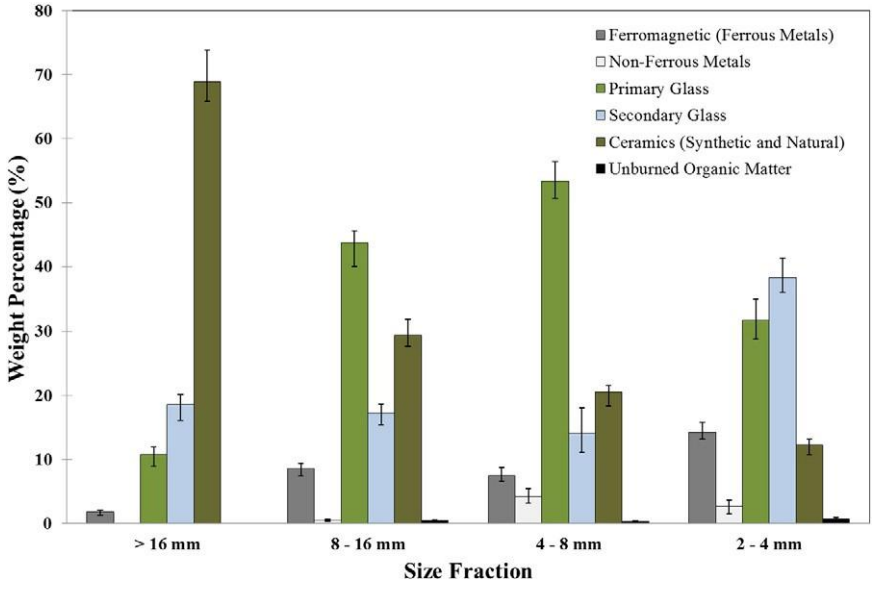

Fig. 7. Distribution of materials as a function of particle size (N 2 mm) in the MSWI bottom ash at the outlet of recovery process at the conditioning plant (sample D).

Table 1
Average results of material contents in the finest fractions of MSWI bottom ash at the outlet of the conditioning plant.

	Size fraction (mm)	
	0–1	1–2
Aluminium (metal)	0.38%	1.16%
Non-ferrous metals[a]	0.51%	1.55%
Ferrous metals	16.31%	19.16%
Organic matter	2.37%	1.67%
Glass (primary and secondary)[b]	60.1%	

[a] Estimated value. It has been considered that the aluminum content accounts for 75% of all nonferrous metals.
[b] Amorphous materials and non-identified crystalline phases.

metals recovered scraps corresponded to metallic aluminium, as previously highlighted by Grosso et al. (2011, 2010) and Biganzoli et al. (2014). The results from the chemical determination of metallic aluminium of sample D for the 1–2 mm and 0–1 mm size fractions were 1.12–1.20 wt% and 0.36–0.40 wt%, respectively (Table 1). A decreasing tendency along decreasing size fractions was observed, being the values obtained in accordance with those from Biganzoli et al. (2013) and Berkhout (2011), who reported ranges of 0.27–0.93 wt% (BA b 1 mm) and 0.26 wt% (0–2 mm) respectively (Berkhout, 2011; Biganzoli et al., 2013). Considering that the percentage of metallic Al in the recovered scrap is between 60 and 90 wt% of the total amount of non-ferrous metals (with an average ≈ 75 wt%), their percentage can be estimated, being 0.51 wt% and 1.55 wt% for 0–1 mm and 1–2 mm size fractions, respectively.

3.2.2.2. Content of glass in the finest fractions. Quantitative phase analysis in the 0–2 mm size fraction was carried out according to Rietveld method. Table 2 describes the content of the crystalline phases. Around 60 wt% is determined as amorphous materials and non-identified crystalline phases, being also calcite and quartz (11.4 and 10.9 wt%, respectively) the prevailing phases. Other minor phases such as ferrous oxides, apatite, feldspar and clay minerals are also present. Assuming that the amorphous phases are mainly due to the presence of glass, it can be estimated that the content of glass (primary and secondary) in this finest fraction is the same as the content in the amorphous phase (60.1 wt%).

3.2.2.3. Content of ferrous metals and organic matter in the finest fractions. Table 1 describes the content of ferrous metals (ferromagnetic metals) and organic matter of two smaller particle size fractions, determined by electromagnets and potassium permanganate oxidation (UNE 103204:93), respectively. It should be noted that the content of ferrous metals in the finest fractions is similar to that determined in the 2–4 mm size fraction, which shows the poor separation efficiency of the electromagnets (MS, Fig. 2) over the small fractions. The high content of magnetite, hematite and wüstite (Table 2), suggests that a ferrous oxide layer coats the finest ferrous particles, which hinders the magnetic attraction forces in the shredding process. The contents of organic matter in the 0–1 and 1–2 mm size fractions were 2.37 and 1.67 wt% respectively. Although the former is slightly higher than the limit of 2% set by the Spanish Technical Specifications for Road Constructions (Section 3.2.1), the relative proportion of the 0–1 mm size fraction in the whole range of size fractions allows expecting a lower value.

Table 2
Quantitative phase analysis in the finest fraction (0–2 mm) of MSWI bottom ash at the outlet of the conditioning plant. Rietveld method by means of FullProf.

Crystalline phases	Percentages in weight (wt%)
Calcite	11.4
Quartz	10.9
Hydrocalumite	6.7
Albite	2.3
Hydroxilapatite	2.1
Magnetite	1.7
Microcline	1.4
Monofluorphosphate apatite	1.1
Hematites	0.9
Muscovite	0.9
Wustite	0.5
Amorphous (and not identified crystalline phases)	60.1

3.3. Distribution of heavy metals

The use of BA is restricted by the release of heavy metals. Among other (pH, weathering grade, neo-formed phases, etc.) their leaching potential is related to its content and mineral form. Fig. 8 shows the content (mg·kg^{-1} of dry matter) of Zn, Pb, Ti, Cu, Mn, Cr, Ni, As, Mo, Cd, Sn, Sb, and Ba for each size fraction at the outlet (sample D). As in the research work carried out in 1999 (Chimenos et al., 1999), the chemical characterization of BA also indicates that the finest fractions contributed significantly to the total heavy metals content. The total metallic aluminium and iron contents are not included in this section since they were considered elsewhere. The results show a decrease in heavy metals content when the main particle size of BA increases. When the metal content for fractions N 4 mm is lower than 1 wt%, the content of 1–2 mm size fractions is higher than 3%. Moreover, like the characterization carried out 15 years ago, Pb, Zn, Cu, Mn and Ti (this last one not formerly determined) showed the highest contribution to the total content of heavy metals (Fig. 8a). While most of the heavy metals reached their maximum content in the 1–2 mm fraction, Zn (boiling point 1180 K) showed this behaviour in the finest fraction, mainly as a result of the vaporisation and condensation processes. The presence of metals in the finest fractions is expected to be comprised of metal oxides (or combined with other anions). Nevertheless, in the fractions higher than 1 mm, they can be found either as metal or metal alloys (e.g. copper wire or lead base alloys for soldering), metal oxide particles adhere to the surface of larger particles, or as additives used in the formulation of ceramics (e.g. TiO_2 as pigment, or $BaTiO_3$ in transducers). According to that, the potential leaching of heavy metals for the fine fractions (i.e. lower than 4 mm) is expected to be higher than the large fractions.

4. Conclusions

A mineralogical and physicochemical characterization was performed on BA as a function of particle size (N 16, 8–16, 4–8, 2–4, 1–2 and 0–1 mm size fractions). This analysis was compared to a similar study carried out by the authors N 15 years ago (1999). The different materials were classified as glass (primary and secondary), ceramics, ferrous metals (ferromagnetic), non-ferrous metals, and unburned matter. Regarding glass, the results show the influence of recycling programs over the last years. On the one hand, the mineralogical analysis of the current BA composition showed a substantial decrease in the total glass weight in particles over 16 mm. This is explained by the fact that entire glass bottles (such as those from beer, wine, and other food and beverage packaging) are easily stored in domestic houses and further collected in the corresponding recycling containers, reducing its presence in BA. Taking into account the relative proportion of each size fraction and their corresponding content of glass (primary and secondary), the amount that is left unrecycled was estimated to be 60.8 wt%. From this value, 26.4 wt% corresponds to primary glass in N 2 mm size fractions. Hence, there is still a significant amount of glass that could be recovered (e.g. curbside collection systems). This unrecovered glass content restricts BA reutilization as secondary road base and subbase material to low traffic roads, due to their elevated fragility and low resistance to fragmentation.

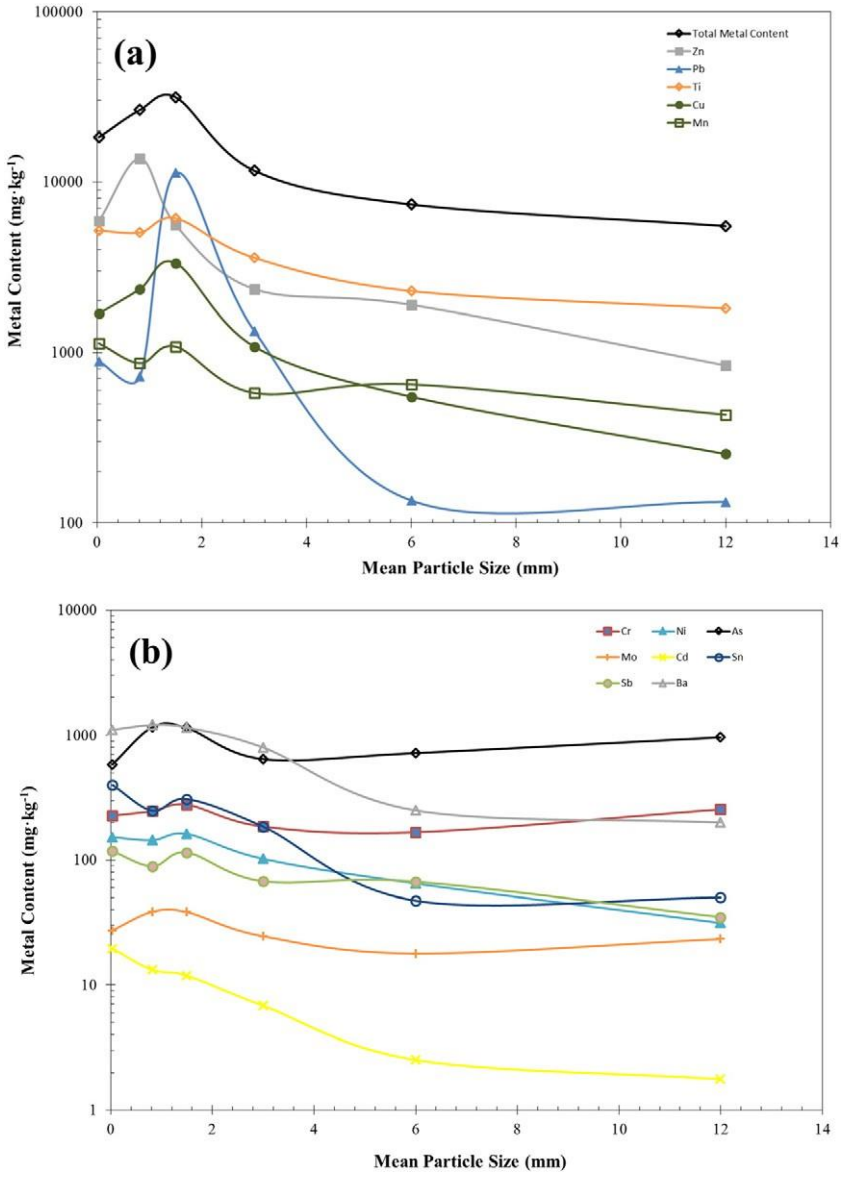

Fig. 8. Distribution of heavy metals as a function of particle size in the BA at the outlet of conditioning plant.

As for the remainder materials, ceramics play a major role in current BA composition since they are not implemented in any specific take-back or voluntary curbside recycling program. Regarding metals, the greatest content of ferromagnetic was observed for the 2–4 mm (N 22 wt%) size fraction while the non-ferrous type was almost non-existent in particles over 16 mm, remaining below 10 wt% for the rest of size fractions. In the finest fractions (b 2 mm), about 60 to 95 wt% of non-ferrous metals corresponded to metallic aluminium. The results from the chemical characterization also indicated that the finest fractions (0–2 mm) contributed significantly (around 73%) to the total heavy metals content, especially for Pb, Zn, Cu, Mn and Ti.

Acknowledgements

The authors would like to thank VECSA (FBG 307133) and SIRUSA (FBG 307131) for their financial support and providing BA samples. Thanks are due to Dr. Xavier Alcobé from the Scientific and Technological Centers at Universitat de Barcelona for his assistance with XRD and Rietveld analysis.

References

AENOR, 1993. UNE 103204:93. Organic Matter Content of a Soil by the Potassium Permanganate Method (Madrid).

ARC, 2016. Agència de Residus de Catalunya. ([WWW Document]. URL http://residus.gencat.cat/es/lagencia/ (accessed 01.01.2016)).

ARPAL, 2012. Estudio sobre la recuperación de envases de aluminio. ([WWW Document]. URL http://aluminio.org/wp-content/uploads/2012/10/Estudio-sobre-la-Recuperacion-de- Envases-de-Aluminio-2011.pdf (acessed 07.01.2016)).

Berkhout, S.P.M., 2011. Optimizing non-ferrous metal value from MSWI bottom ashes. J. Environ. Prot. 02:564–570 (Irvine,. Calif). http://dx.doi.org/10.4236/jep.2011.25065.

Biganzoli, L., Grosso, M., 2013. Aluminium recovery from waste incineration bottom ash, and its oxidation level. Waste Manag. Res. 31, 954–959.

Biganzoli, L., Grosso, M., Forte, F., 2014. Aluminium mass balance in waste incineration and recovery potential from the bottom ash: a case study. Waste Biomass Valoriz. 5, 139–145.

Biganzoli, L., Ilyas, A., Praagh, M.V., Persson, K.M., Grosso, M., 2013. Aluminium recovery vs. hydrogen production as resource recovery options for fine MSWI bottom ash fraction. Waste Manag. 33, 1174–1181.

Bontempi, E., Zacco, A., Borgese, L., Gianoncelli, A., Ardesi, R., Depero, L.E., 2010. A new method for municipal solid waste incinerator (MSWI) fly ash inertization, based on colloidal silica. J. Environ. Monit. 12, 2093–2099.

Chandler, A.J., Eighmy, T.T., Hjelmar, O., Kosson, D.S., Sawell, S.E., Vehlow, J., van der Sloot, H.A., Hartlén, J., 1997. Municipal Solid Waste Incinerator Residues Studies in Environmental Sciences. Elsevier Science Publishers B.V.

Chimenos, J., Segarra, M., Fernández, M., Espiell, F., 1999. Characterization of the bottom ash in municipal solid waste incinerator. J. Hazard. Mater. 64:211–222. http://dx.doi.org/10.1016/S0304-3894(98)00246-5.

Chimenos, J.M., Fernández, A.I., Miralles, L., Segarra, M., Espiell, F., 2003. Short-term natural weathering of MSWI bottom ash as a function of particle size. Waste Manag. 23, 887–895 (doi:S0956-053X(03)00074-6).

Eurostat, 2016. Packaging Waste Statistics - Statistics Explained. ([WWW Document]. URL http://epp.eurostat.ec.europa.eu/statistics_explained/index.php/Packaging_waste_statistics# (accessed 07.01.2016)).

Freyssinet, P., Piantone, P., Azaroual, M., Itard, Y., Clozel-Leloup, B., Guyonnet, D., Baubron, J.C., 2002. Chemical changes and leachate mass balance of municipal solid waste bottom ash submitted to weathering. Waste Manag. 22, 159–172.

Ginés, O., Chimenos, J.M., Vizcarro, A., Formosa, J., Rosell, J.R., 2009. Combined use of MSWI bottom ash and fly ash as aggregate in concrete formulation: environmental and mechanical considerations. J. Hazard. Mater. 169:643–650. http://dx.doi.org/10.1016/j.jhazmat.2009.03.141.

Grosso, M., Biganzoli, L., Rigamonti, L., 2011. A quantitative estimate of potential aluminium recovery from incineration bottom ashes. Resour. Conserv. Recycl. 55, 1178–1184. Grosso, M., Rigamonti, L., Biganzoli, L., Schiona, G., 2010. Metals Recovery From Incineration Bottom Ashes: Future Opportunities in Italy 1–9.

Hu, Y., Bakker, M.C.M., de Heij, P.G., 2011. Recovery and distribution of incinerated aluminum packaging waste. Waste Manag. 31, 2422–2430.

ICDD, 2006. International Centre for Diffraction Data - PDF-2 Powder.

Izquierdo, M., López-Soler, A., Ramonich, E.V., Barra, M., Querol, X., 2002. Characterisation of bottom ash from municipal solid waste incineration in Catalonia. J. Chem. Technol. Biotechnol. 77, 576–583.

Miller, C., 1995. Waste product profiles. In: Aquino, J.T. (Ed.), Waste Age/Recycling Time's Recycling Handbook. Environmental Industry Associations, pp. 1–4.

Ministerio de Fomento, 2010. Pliego de prescripciones técnicas generales para obras de carreteras y puentes PG3 (Madrid).

Monteiro, R.C.C., Alendouro, S.J.G., Figueiredo, F.M.L., Ferro, M.C., Fernandes, M.H.V., 2006. Development and properties of a glass made from MSWI bottom ash. J. Non-Cryst. Solids 352, 130–135.

PRECAT20, 2012. Programa general de prevenció i gestió de residus i recursos de Catalunya 2013–2020 (Spain).

Puma, S., Marchese, F., Dominijanni, A., Manassero, M., 2013. Reuse of MSWI bottom ash mixed with natural sodium bentonite as landfill cover material. Waste Manag. Res. 31, 577–584.

Rietveld, H.M., 1969. A profile refinement method for nuclear and magnetic structures. J. Appl. Crystallogr. 2, 65–71.

Roy, N.U., 1996. Recycling realities and the glass container: new technologies and trends. In: Rebers, A., R.E.L., P. (Eds.), Municipal Solid Wastes Problems and Solutions. CRC Press LLC, pp. 1–9.

Tchobanoglous, G., Theisen, H., Vigil, S., 1994. Integrated Solid Waste Management Engineering Principles and Management Issues. first edit. ed. McGraw-Hill, Inc.

Ward, C.R., French, D., 2006. Determination of glass content and estimation of glass composition in fly ash using quantitative X-ray diffractometry. Fuel 85:2268–2277. http://dx.doi.org/10.1016/j.fuel.2005.12.026.

Wei, Y., Shimaoka, T., Saffarzadeh, A., Takahashi, F., 2011. Mineralogical characterization of municipal solid waste incineration bottom ash with an emphasis on heavy metal-bearing phases. J. Hazard. Mater. 187, 534–543.

Zevenbergen, C., Van Reeuwijk, L.P., Bradley, J.P., Bloemen, P., Comans, R.N.J., 1996. Mechanism and conditions of clay formation during natural weathering of MSWI bottom ash. Clay Clay Miner. 44, 546–552.

Zhou, B., Yang, Y., Reuter, M.A., Boin, U.M.J., 2006. Modelling of aluminium scrap melting in a rotary furnace. Miner. Eng. 19, 299–308.